Supporting Information

Cells adhering to 3D nanoscales: Cell membrane reshaping without stable internalization

Michele Dipalo[‡a], Allister F. McGuire[‡c], Hsin-Ya Lou[c], Valeria Caprettini[a†], Giovanni Melle[a], Giulia Bruno[a], Claudia Lubrano[b], Laura Matino[b], Francesco De Angelis[a], Bianxiao Cui*[c] and Francesca Santoro*[b]*

Table of Contents

Experimental Procedure

Nanostructures fabrication: STPs and STCs were fabricated on thin silicon nitride membranes by means of a focused ion beam (FIB) milling technique[1]. The nanostructures consist of a polymeric scaffold coated with a thin layer of gold. Quartz pillars were fabricated by electron beam lithography and reactive ion etching as reported previously[2,3].

MEA fabrication: STPs and STCs on MEA were fabricated according to the FIB-based method introduced in a previous work[4]. SSP and IrOx nanotubes on MEA were fabricated via electrodeposition[5] and final devices are similar to those in previous work[6].

Cell culture: After 20 min. of UV irradiation, the substrates were treated with poly-L-lysine 0.01% w/v (Sigma-Aldrich) for five minutes, washed extensively with water and allowed to dry in sterile conditions. Subsequently, HL-1 cells[7] have been seeded at a density of 35000/cm^2 and grown with Claycomb culture medium, supplemented with 10% fetal bovine serum, 100 µM norepinephrine, 300 µM ascorbic acid, 2 mM L-glutamine and penicillin and streptomycin (Sigma-Aldrich).

Cell Staining: Cells were fixed in glutaraldehyde 2.5% in sodium cacodylate 0.1 M pH 7.4 buffer for 2 h at room temperature. A first staining in glycine 20 mM in buffer solution was performed to reduce the signal to noise ratio, saturating the nonspecific signal, and a three step protocol (reduced osmium, thiocarbohydrazide, osmium (RO-T-O) in aqueous solution) recently developed[8,9] was applied to the samples. The heavy staining of the cell membranes provided by this protocol, allows for a clear imaging of the lipid membranes at the interface with the 3D nanostructures. An overnight negative staining with 5% uranyl acetate in aqueous solution was performed, followed by 3 min. in tannic acid to stain the cytoskeleton. Dehydration in increasing concentration of ethanol was performed, followed by embedding in increasing concentration of Spurr resin. The excess of resin was removed with rapid washes in ethanol before overnight polymerization at 65 °C. After polymerization, the specimens were metalized with a thin layer of gold (10 nm) and mounted on a standard SEM/FIB stub with silver paste.

SEM/FIB imaging: The cross-sectioning and imaging were performed with a dual beam Helios Nanolab600 by ThermoFisher equipped with a gas injection system. The region of interest of the samples (i.e., the cells at the interface with the 3D nanostructures) was coated with a protective layer of Pt with an electron-assisted deposition followed by an ion-assisted deposition. Trenches were milled with ions accelerated at 30 kV with a current of 0.79 nA, and

a polishing cross section was performed. Images of the cross section were acquired with the sample tilted at 52° (perpendicular to the ion beam) collecting the backscattered electrons using a through-lens detector. Beam current and acceleration voltage were respectively 0.40 nA and 3 kV.

Electrophysiology: Electrical recordings on MEAs with STPs and STCs have been performed on a custom acquisition system based on the amplifier chip RHA2132 from Intan Technologies. Further details about the custom system are available on our previous work[10].

Fluorescence: Quartz chips patterned with nanostructures were coated with 0.1 mg/mL poly-L-lysine overnight at 37 ºC. HEK293 cells transfected with CAAX-mCherry were then plated on the structures and cultured in Dulbecco's Modified Eagle's Medium (DMEM) with 10% v/v fetal bovine serum. After a predetermined time (usually 4 h or 24 h), the cultures were exposed to 10 μM calcein in DMEM for 10 min., the calcein was washed out, and fresh DMEM added. The cells' epifluorescence was imaged in an inverted microscope.

Supplemental figures

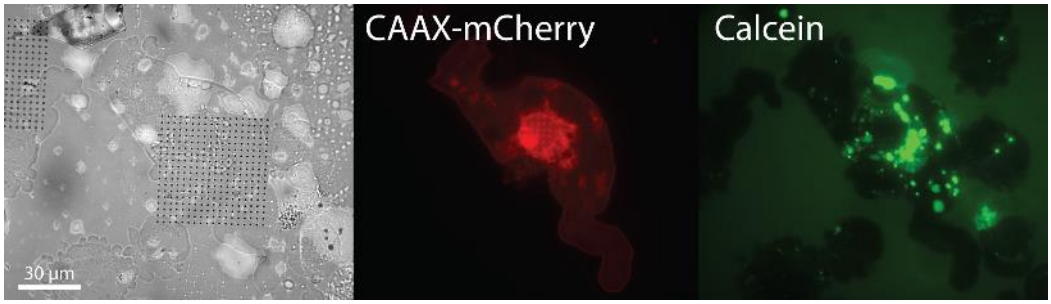

Supplemental Figure 1: Positive calcein signal due to HL-1 membrane permeabilization after apoptosis. Image on tall nanocones, 8 h after plating.

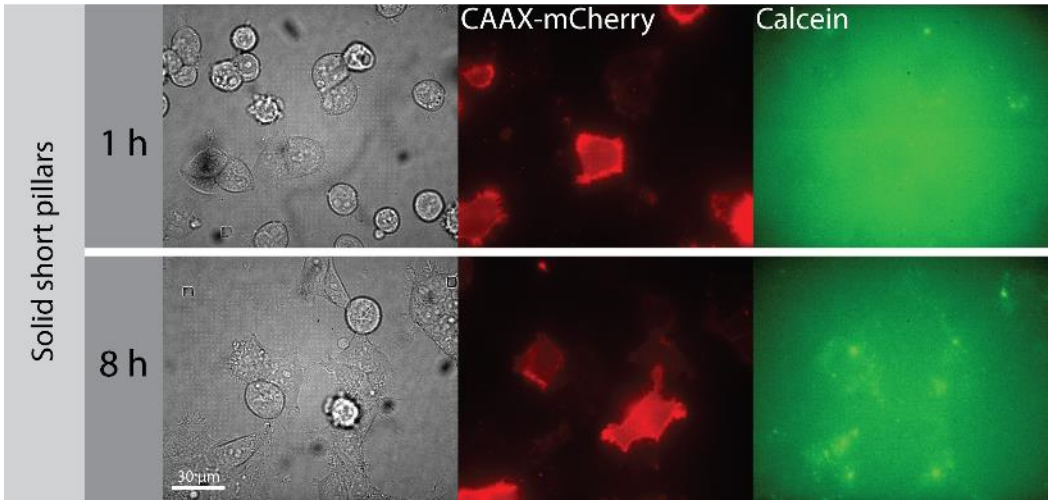

Supplemental Figure 2: Short nanopillars at early time points 1 h and 8 h after plating.

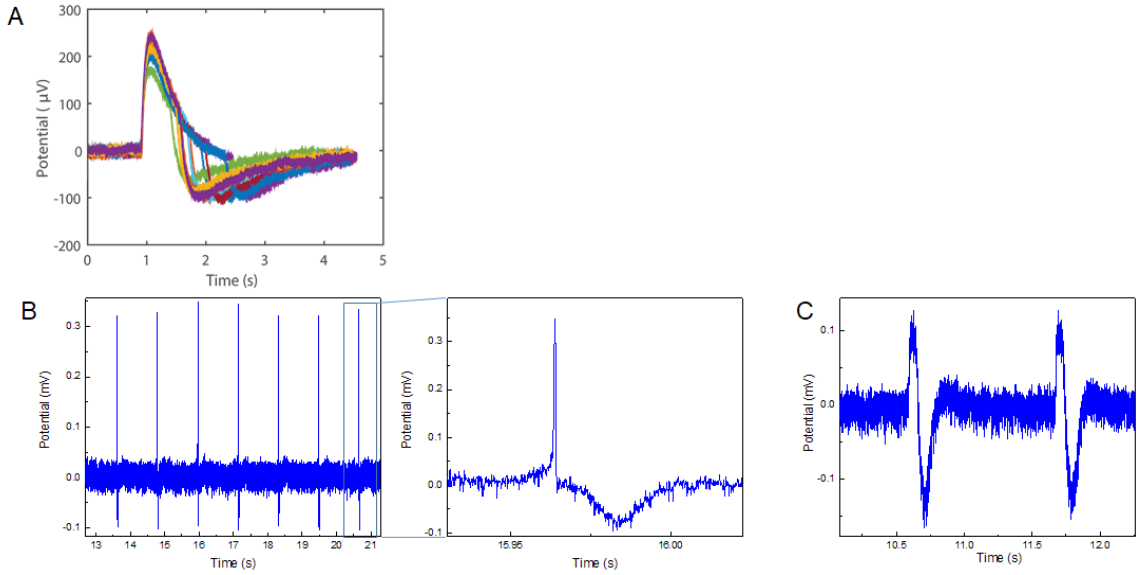

Supplemental Figure 3: A: Rare example of spiking HEK cells on sharp IrOx nanotubes yielding spontaneous action potentials, DIC1. B: Rare example of spiking HL-1 cells on sharp nanopillars with partial intracellular coupling. C: The same cell as in panel B after electroporation. The signal acquires longer duration as expected for a more pronounced intracellular coupling.

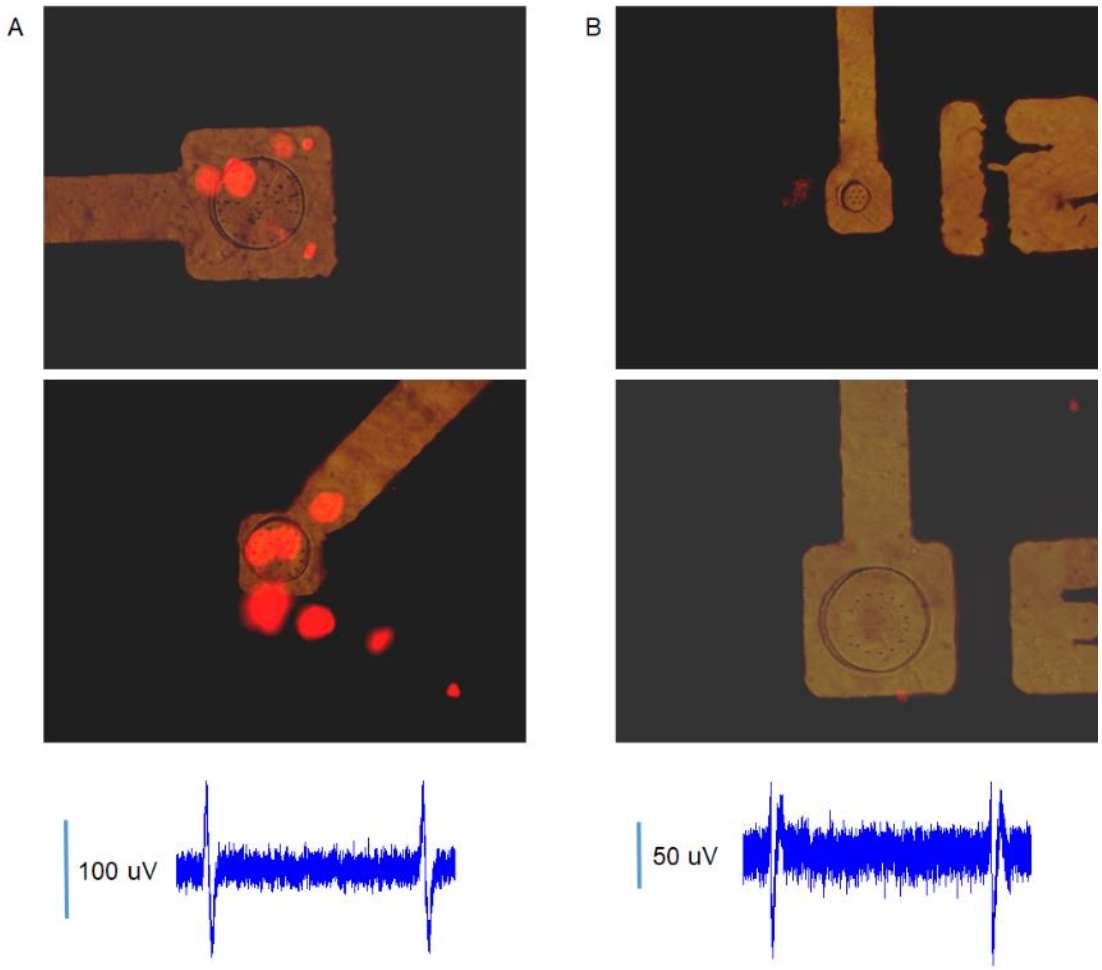

Supplemental Figure 4: Bright field and red fluorescence superimposed images of HL-1 on MEA with sharp nanopillars after electroporation (A) and in electrophysiological conditions (B) with Propidium Iodide in the cell medium. On the bottom, exemplary recordings in the two cases are reported, respectively intracellular (A) and extracellular (B).

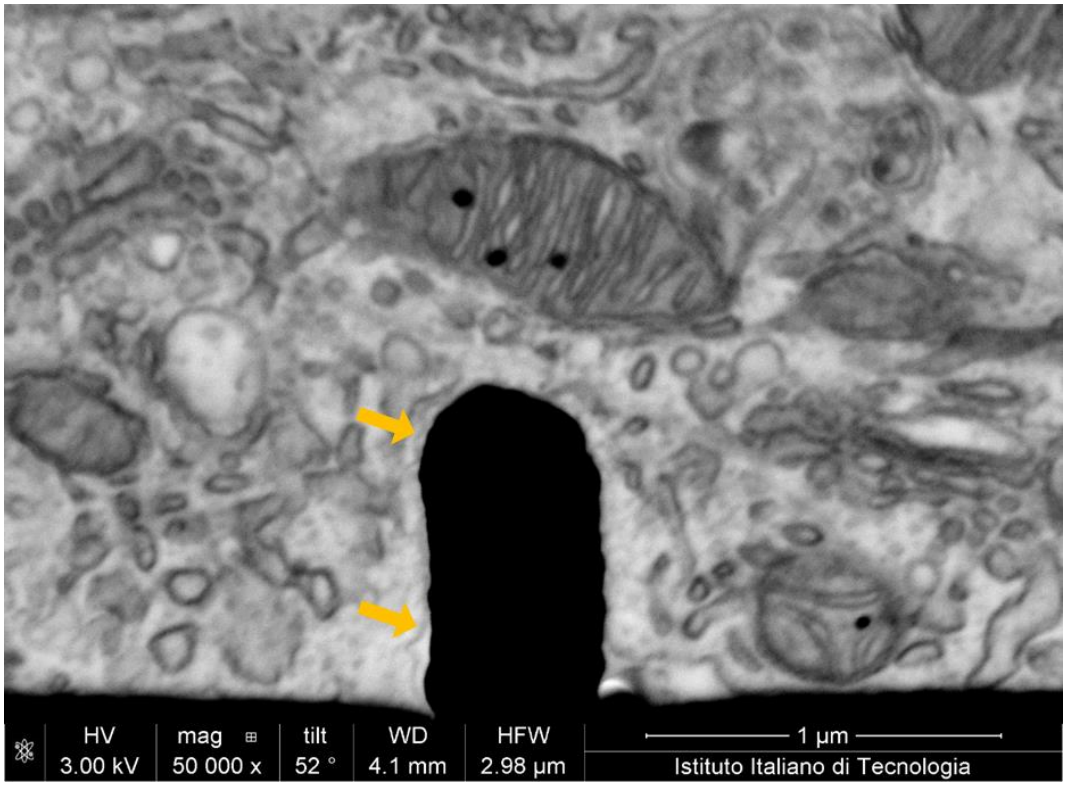

Supplemental Figure 5: Enlarged view of HL-1 cell on short nanopillar fixated at 4h.

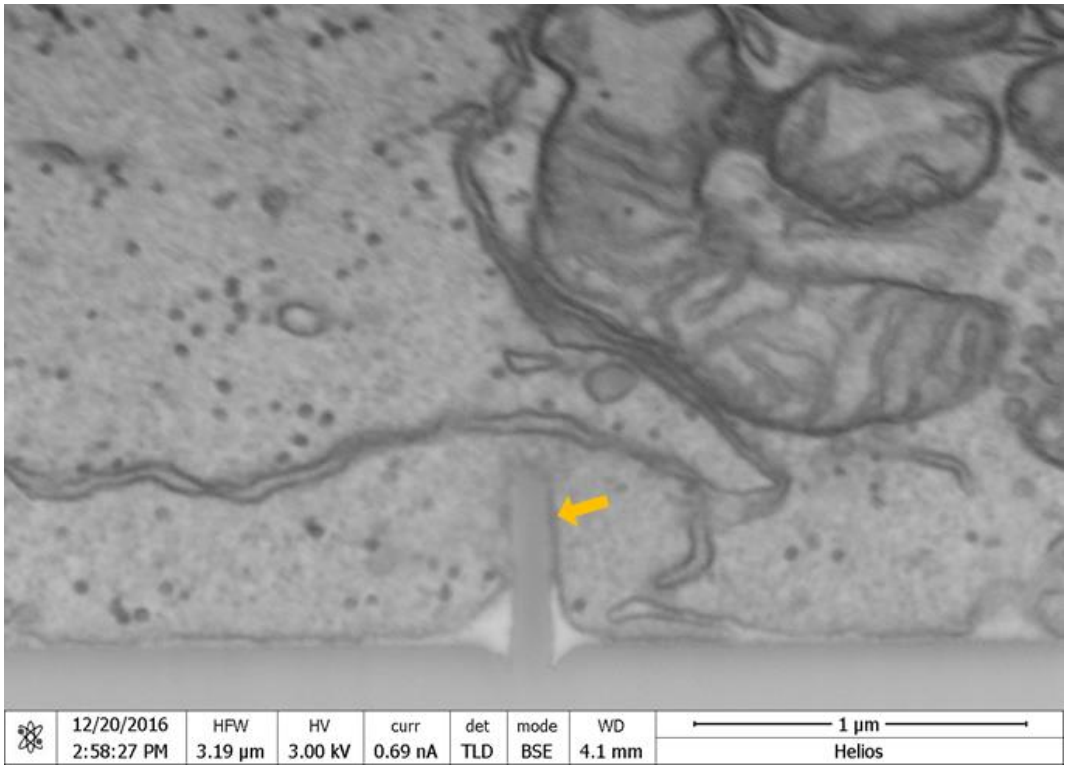

Supplemental Figure 6: Enlarged view of HL-1 cell on short nanopillar fixated at 24h.

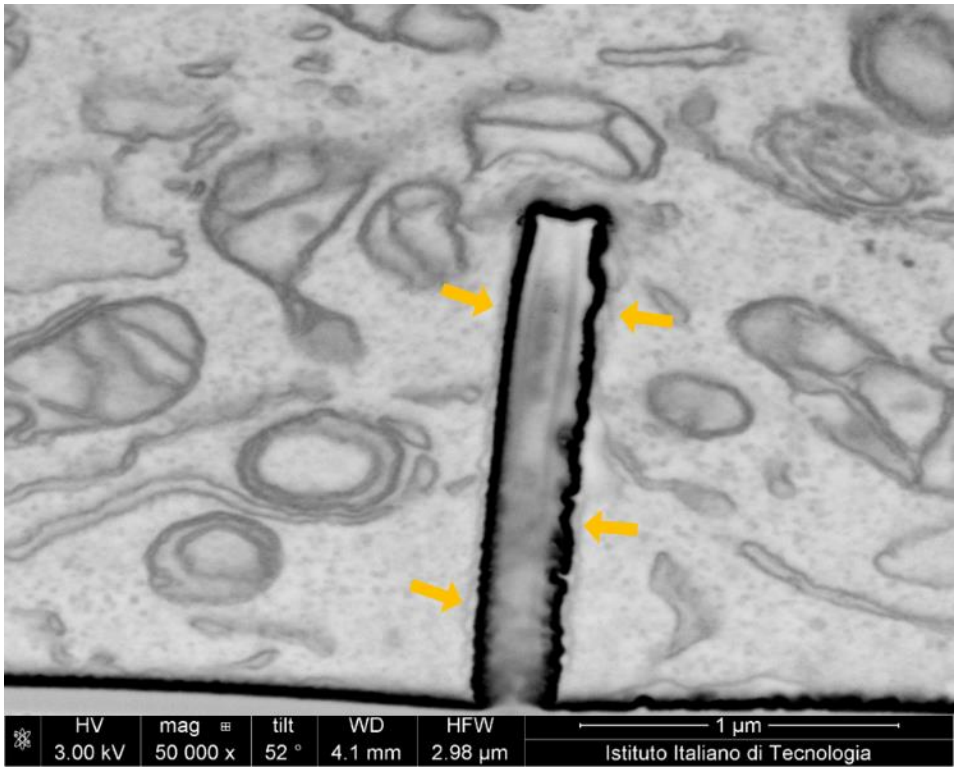

Supplemental Figure 7: Enlarged view of HL-1 cell on tall nanopillar fixated after 4h.

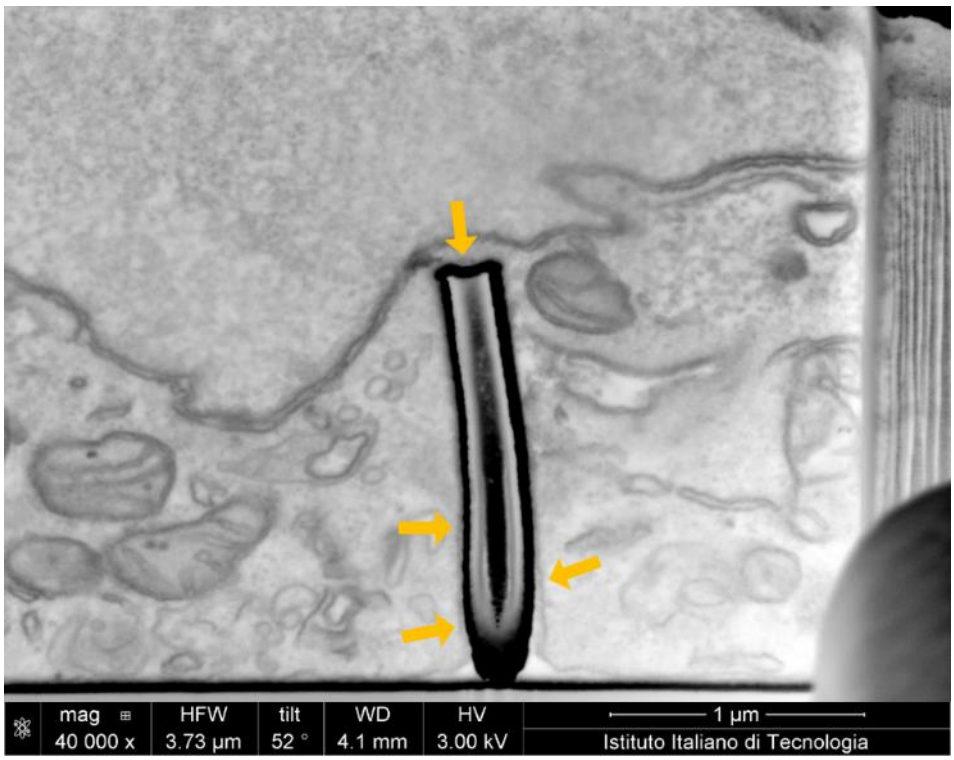

Supplemental Figure 8: Enlarged view of HL-1 cell on tall nanopillar fixated at 24h

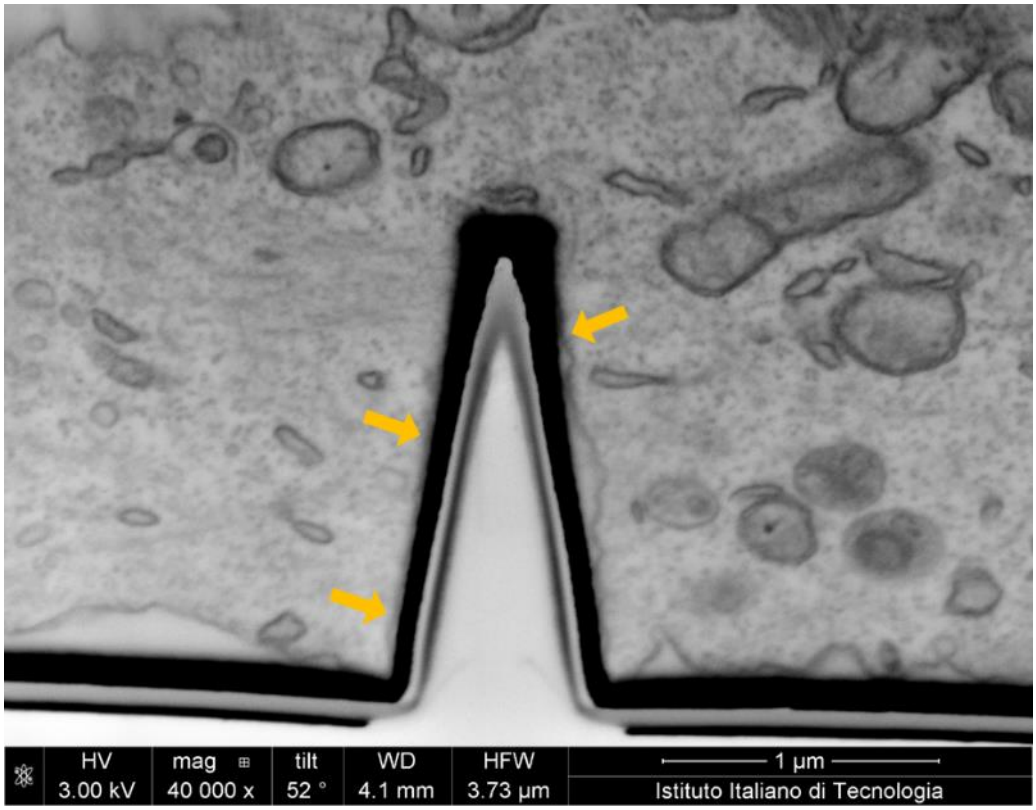

Supplemental Figure 9: Enlarged view of HL-1 cell on nanocone fixated at 4h.

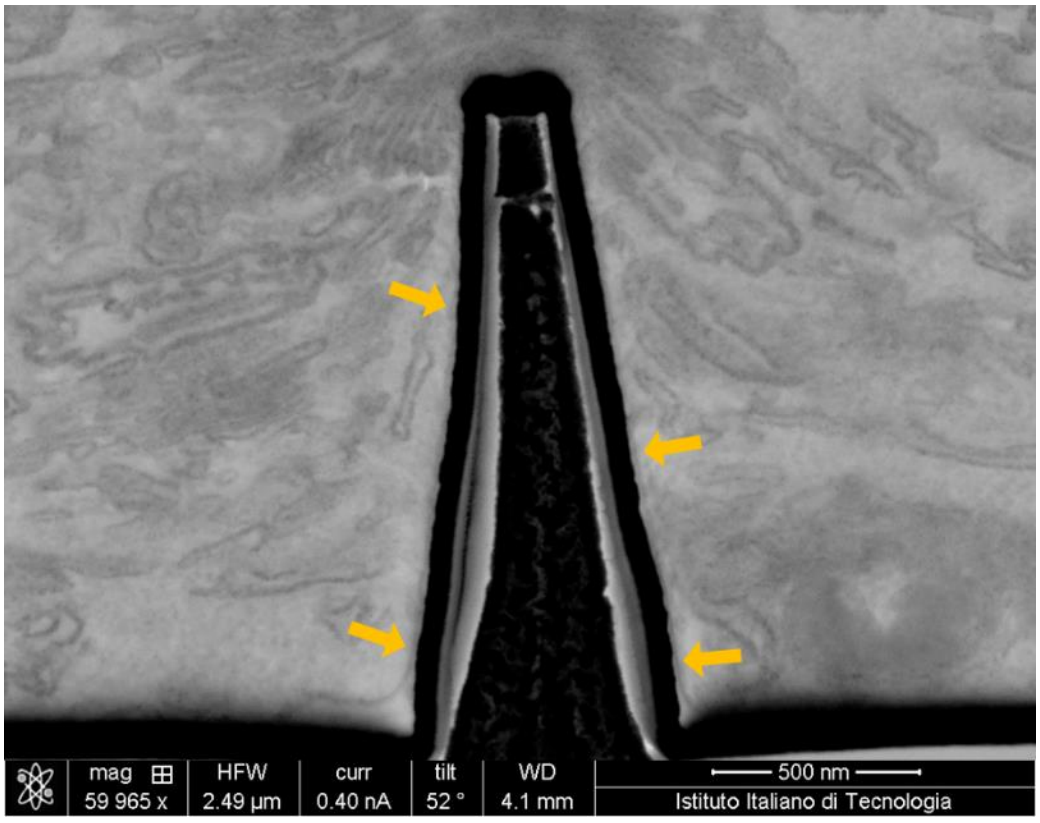

Supplemental Figure 10: Enlarged view of HL-1 cell on nanocone fixated at 24h.

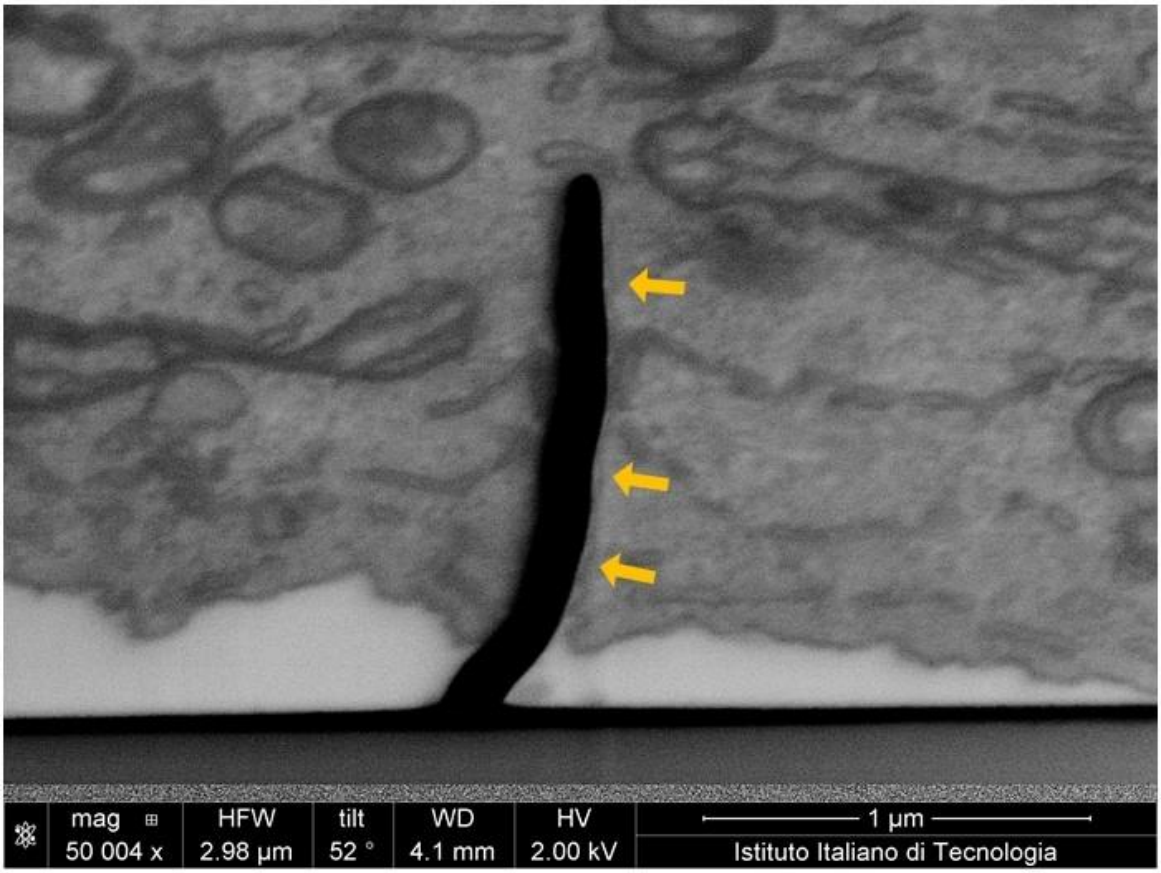

Supplemental Figure 11: Enlarged view of HL-1 cell on sharp nanopillars fixated at 4h.

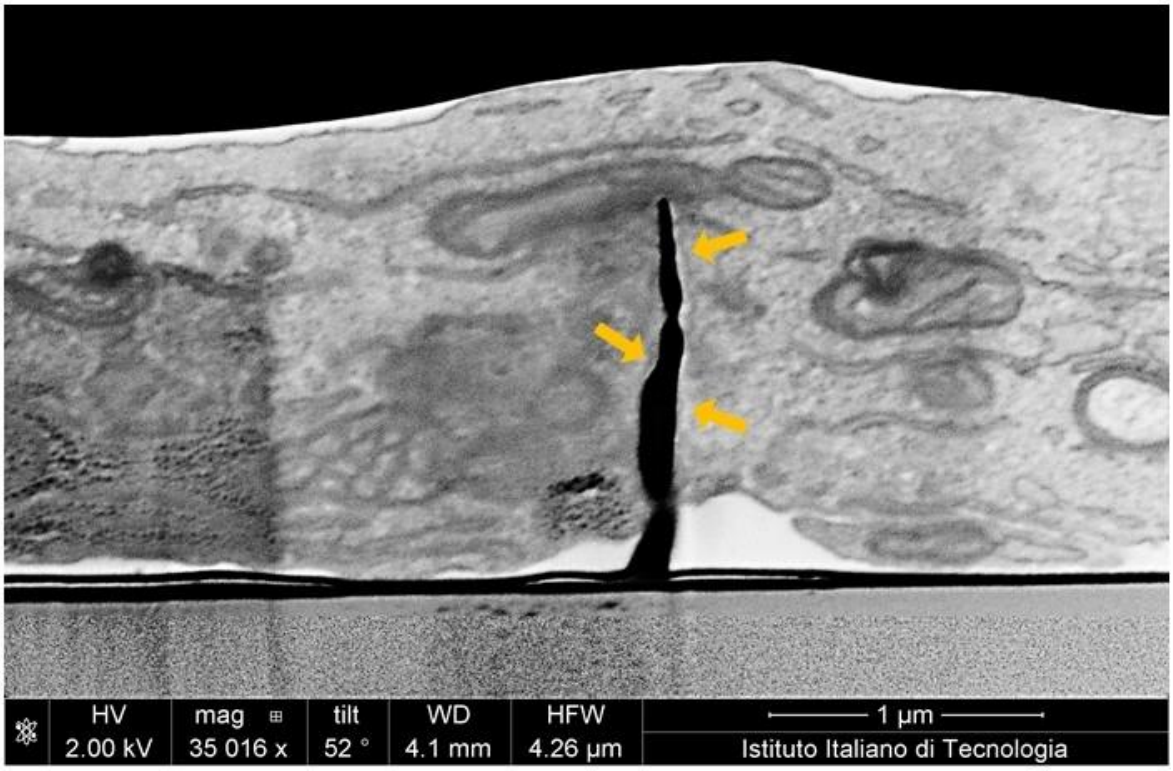

Supplemental Figure 12: Enlarged view of HL-1 cell on sharp nanopillars fixated at 24h.

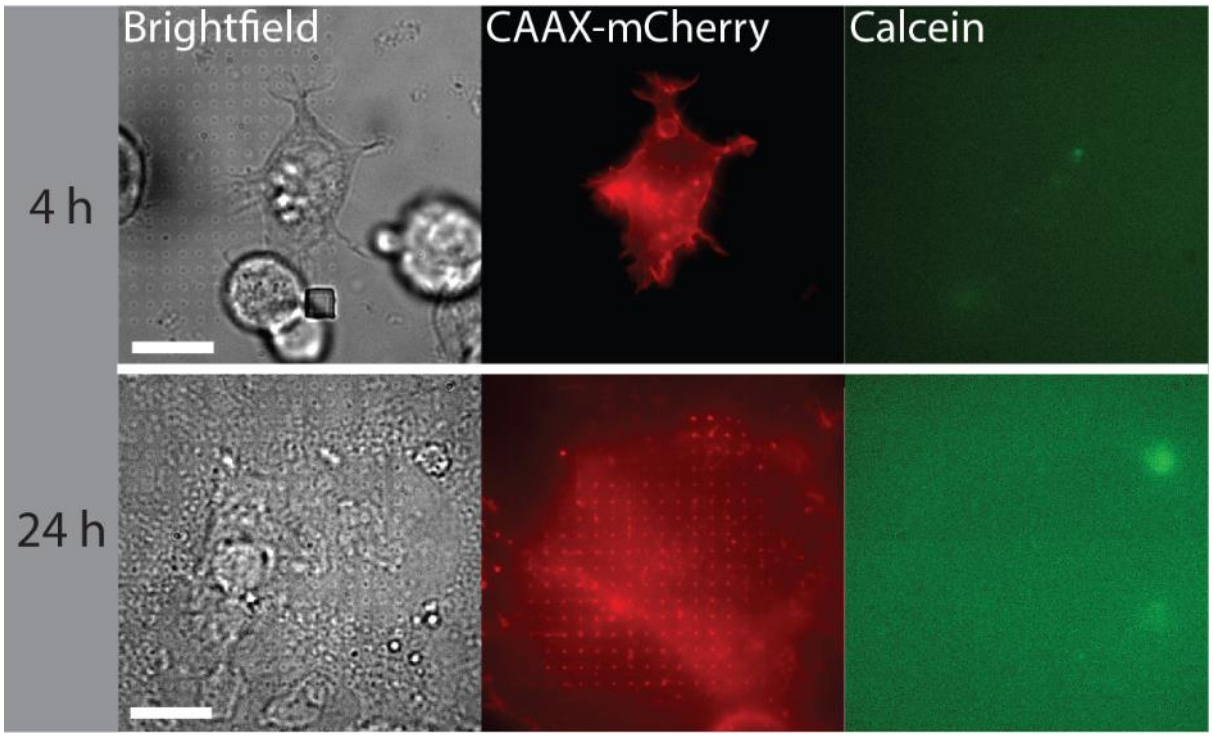

Supplemental Figure 13: Enlarged images of CAAX-mCherry-transfected HEK cells on SSPs.

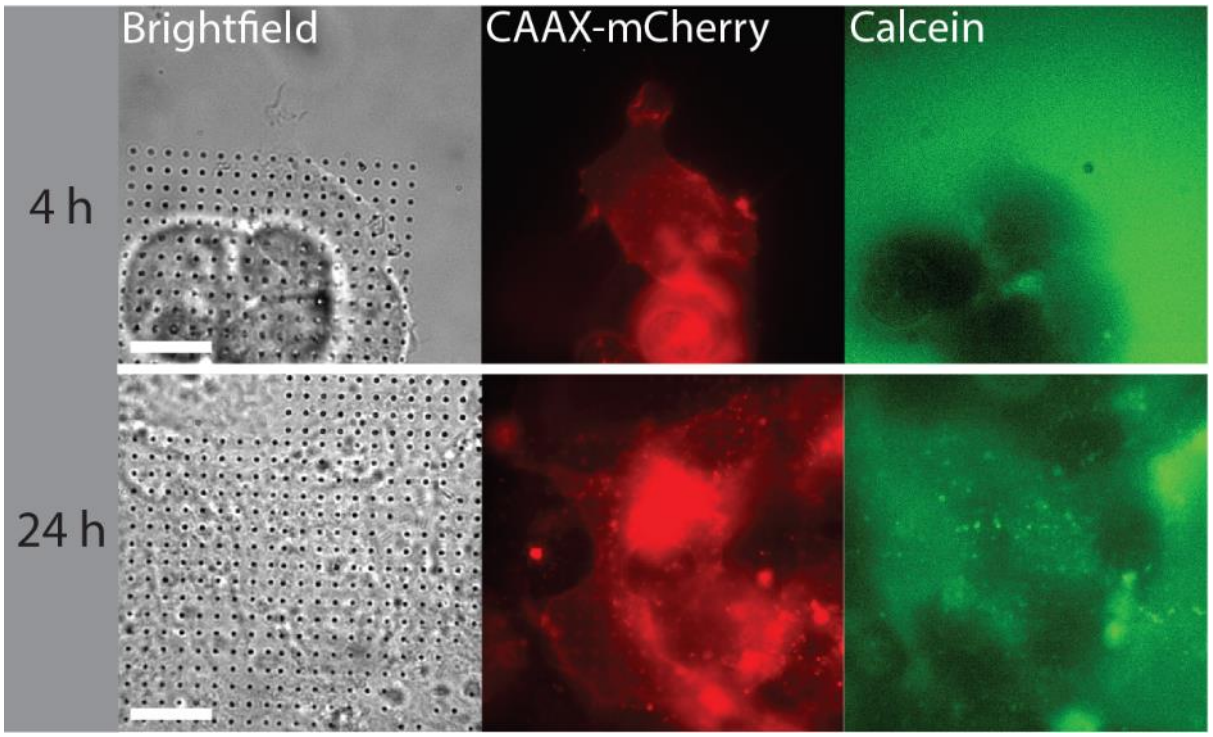

Supplemental Figure 14: Enlarged images of CAAX-mCherry-transfected HEK cells on STPs.

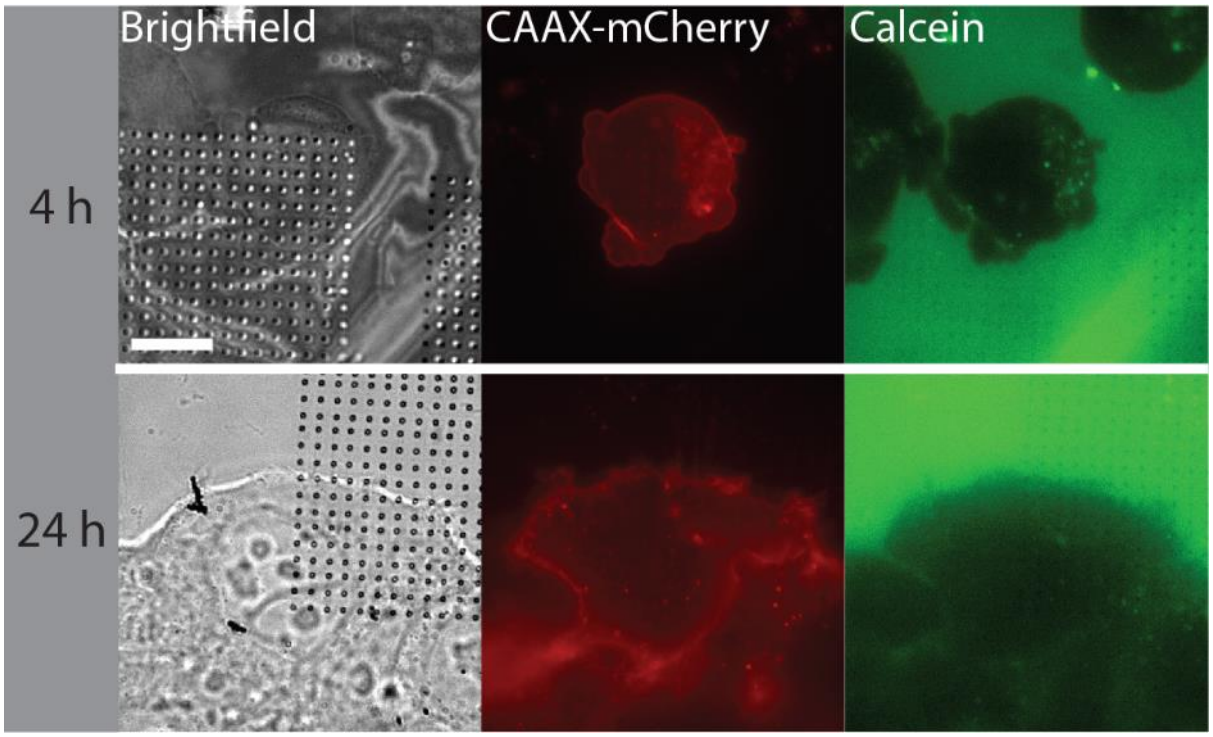

Supplemental Figure 15: Enlarged images of CAAX-mCherry-transfected HEK cells on STCs.

REFERENCES

(1) De Angelis, F.; Malerba, M.; Patrini, M.; Miele, E.; Das, G.; Toma, A.; Zaccaria, R. P.; Di Fabrizio, E. 3D Hollow Nanostructures as Building Blocks for Multifunctional Plasmonics. *Nano Lett.* **2013**, *13*, 3553–3558.

(2) Hanson, L.; Zhao, W.; Lou, H. Y.; Lin, Z. C.; Lee, S. W.; Chowdary, P.; Cui, Y.; Cui, B. Vertical Nanopillars for in Situ Probing of Nuclear Mechanics in Adherent Cells. *Nat. Nanotechnol.* **2015**, *10* (6), 554–562.

(3) Zhao, W.; Hanson, L.; Lou, H.-Y.; Akamatsu, M.; Chowdary, P. D.; Santoro, F.; Marks, J. R.; Grassart, A.; Drubin, D. G.; Cui, Y.; et al. Nanoscale Manipulation of Membrane Curvature for Probing Endocytosis in Live Cells. *Nat. Nanotechnol.* **2017**, *12* (8), 750–756.

(4) Dipalo, M.; Messina, G. C.; Amin, H.; La Rocca, R.; Shalabaeva, V.; Simi, A.; Maccione, A.; Zilio, P.; Berdondini, L.; De Angelis, F. 3D Plasmonic Nanoantennas Integrated with MEA Biosensors. *Nanoscale* **2015**, *7*, 3703–3711.

(5) Shmoel, N.; Rabieh, N.; Ojovan, S. M.; Erez, H.; Maydan, E.; Spira, M. E. Multisite Electrophysiological Recordings by Self-Assembled Loose-Patch-like Junctions between Cultured Hippocampal Neurons and Mushroom-Shaped Microelectrodes. *Sci. Rep.* **2016**, *6*, 27110.

(6) Lin, Z. C.; Xie, C.; Osakada, Y.; Cui, Y.; Cui, B. Iridium Oxide Nanotube Electrodes for Sensitive and Prolonged Intracellular Measurement of Action Potentials. *Nat. Commun.* **2014**, *5*, 3206.

(7) Claycomb, W. C.; Jr, N. A. L.; Stallworth, B. S.; Egeland, D. B.; Delcarpio, J. B.; Bahinski, A.; Jr, N. J. I. HL-1 Cells: A Cardiac Muscle Cell Line That Contracts and Retains Phenotypic Characteristics of the Adult Cardiomyocyte. *Proc. Natl. Acad. Sci. USA* **1998**, *95* (6), 2979–2984.

(8) Belu, A.; Schnitker, J.; Bertazzo, S.; Neumann, E.; Mayer, D.; OffenhÄusser, A.; Santoro, F. Ultra-Thin Resin Embedding Method for Scanning Electron Microscopy of Individual Cells on High and Low Aspect Ratio 3D Nanostructures. *J. Microsc.* **2016**, *263* (1), 78–86.

(9) Santoro, F.; Zhao, W.; Joubert, L.-M.; Duan, L.; Schnitker, J.; van de Burgt, Y.; Lou, H.-Y.; Liu, B.; Salleo, A.; Cui, L.; et al. Revealing the Cell–Material Interface with Nanometer Resolution by Focused Ion Beam/Scanning Electron Microscopy. *ACS Nano* **2017**, *11* (8), 8320–8328.

(10) Dipalo, M.; Amin, H.; Lovato, L.; Moia, F.; Caprettini, V.; Messina, G. C.; Tantussi, F.; Berdondini, L.; De Angelis, F.; Angelis, F. De. Intracellular and Extracellular Recording of Spontaneous Action Potentials in Mammalian Neurons and Cardiac Cells with 3D Plasmonic Nanoelectrodes. *Nano Lett.* **2017**, *17* (6), 3932–3939.